

Electric ring currents in atomic orbitals and magnetic fields induced by short intense circularly polarized π laser pulses

Ingo Barth* and Jörn Manz

Institut für Chemie und Biochemie, Freie Universität Berlin, Takustr. 3, 14195 Berlin, Germany
and Kavli Institute for Theoretical Physics, University of California, Santa Barbara, California 93106-4030, USA
 (Received 19 October 2006; published 31 January 2007)

Electric ring currents I_{nlm} and corresponding magnetic fields \mathbf{B}_{nlm} exist in atomic orbitals ψ_{nlm} ($m \neq 0$). Simple expressions are derived for I_{nlm} and for $\mathbf{B}_{nlm}(\mathbf{r}=\mathbf{0})$ at the nucleus. The magnitude of I_{nlm} depends only on n and decreases with increasing quantum number n . In contrast, $\mathbf{B}_{nlm}(\mathbf{r}=\mathbf{0})$ decreases with increasing quantum numbers n and l but increases with m . The largest magnitudes of the electric ring currents and induced magnetic fields are thus obtained for $2p_{\pm 1}$ orbitals. Moreover, I_{nlm} and $\mathbf{B}_{nlm}(\mathbf{r}=\mathbf{0})$ increase with the nuclear charge Z as Z^2 and Z^3 , respectively. Simple circularly polarized π laser pulses are designed for complete population transfers from $1s$ to target $2p_{\pm 1}$ orbitals. The corresponding solutions of the time-dependent Schrödinger equation for the hydrogen atom H ($Z=1$) imply equivalent solutions for arbitrary Z , by means of simple scaling laws for the time ($1/Z^2$), frequency (Z^2), and field strength (Z^3) or intensity (Z^6). For example, the parameters of the π pulse for H (pulse duration $\tau=115$ fs, maximum intensity $\mathcal{I}_{\max}=1.47 \times 10^{10}$ W cm $^{-2}$) are scaled to values $\tau=679$ as and $\mathcal{I}_{\max}=7.09 \times 10^{16}$ W cm $^{-2}$ for Al $^{12+}$, inducing the giant magnetic field $|\mathbf{B}_{21\pm 1}(\mathbf{r}=\mathbf{0})|=1146$ T. The results for hydrogenlike atoms allow corresponding estimates of electric ring currents and magnetic fields in molecules, where molecular orbitals are expressed as linear combinations of atomic orbitals.

DOI: 10.1103/PhysRevA.75.012510

PACS number(s): 32.10.-f, 32.80.Qk

I. INTRODUCTION

Recently we discovered that short circularly polarized laser pulses with durations τ in the femtosecond (fs) or subfemtosecond/attosecond (as) domain can induce strong electron circulations [1–3] or electronic ring currents [4,5] in oriented molecules with rotational symmetries supporting degenerate electronic excited states. These ring currents in turn induce strong magnetic fields $\mathbf{B}(\mathbf{r}=\mathbf{0})$ at the center ($\mathbf{r}=\mathbf{0}$). For example, an optimized so-called π pulse with duration $\tau=3.52$ fs, carrier frequency $\omega=3.42$ eV/ \hbar , and maximum intensity $\mathcal{I}_{\max}=1.28 \times 10^{12}$ W cm $^{-2}$ induces the ring current $I=84.5$ μ A and the magnetic field $|\mathbf{B}(\mathbf{r}=\mathbf{0})|=0.159$ T in oriented Mg-porphyrin (MgP) [4]. For comparison, the traditional approach would require an external static magnetic field of 8048 T to induce the same electric ring current in MgP, a magnitude far beyond the reach of present technology [6,7]. Extended investigations show that the phenomena are even more dramatic in smaller molecules. For example, a circularly polarized optimized π pulse with parameters $\tau=2.5$ fs, $\omega=4.65$ eV/ \hbar , and $\mathcal{I}_{\max}=8.68 \times 10^{12}$ W cm $^{-2}$ can excite a toroidal electric ring current $I \approx 400$ μ A in the oriented diatomic molecule AlCl, thus generating a magnetic field $|\mathbf{B}(\mathbf{r}=\mathbf{R}_{\text{Al}})| \approx 7.7$ T at the Al nucleus [5]. It was suggested that these effects also be investigated in atoms or atomic ions where one might expect, by extrapolation, even stronger effects [8]. The purpose of the present paper is thus to develop the theory of electric ring

currents I_{nlm} and induced magnetic fields $\mathbf{B}_{nlm}(\mathbf{r}=\mathbf{0})$ at the nucleus of hydrogenlike systems with atomic orbitals ψ_{nlm} . We shall derive simple analytical expressions for I_{nlm} and $\mathbf{B}_{nlm}(\mathbf{r}=\mathbf{0})$. These allow us to determine the atomic orbitals ψ_{nlm} with maximum values of I_{nlm} and $|\mathbf{B}_{nlm}(\mathbf{r}=\mathbf{0})|$ depending on the quantum numbers n, l, m and the nuclear charge Z . These selective atomic orbitals then serve as target states for excitation by means of circularly polarized π pulses from the ground state ψ_{100} ($1s$ orbital). We shall show that very strong electric ring currents and giant magnetic fields $|\mathbf{B}_{nlm}(\mathbf{r}=\mathbf{0})| \gg 100$ T can indeed be induced by means of intense ultrashort laser pulses, with durations from attoseconds (as) to femtoseconds (fs), depending on Z . For simplicity, we restrict the derivation to the nonrelativistic regime of the laser pulses (i.e., $\mathcal{I}_{\max} \leq 10^{18}$ W cm $^{-2}$). As we shall show, this implies restrictions to applications to ions with modest nuclear charges, e.g., $Z \leq 13$, depending on the durations of the laser pulses. Relativistic effects will be considered, nevertheless, for the determination of the optimal laser frequencies ω as a function of Z .

Sections II and III present the derivation of the electric ring currents I_{nlm} and the induced magnetic fields $\mathbf{B}_{nlm}(\mathbf{r}=\mathbf{0})$ at the nuclei with charge Ze . For comparison, Sec. IV presents an approximate expression of $\mathbf{B}_{nlm}(\mathbf{r}=\mathbf{0})$, based on a loop ring model of electrons circulating around the nucleus with mean radius R_{nlm} . The results of Secs. II and III, confirmed by Sec. IV, allow the selection of atomic orbitals ψ_{nlm} with maximum values of I_{nlm} and $|\mathbf{B}_{nlm}(\mathbf{r}=\mathbf{0})|$. Section V discusses the design of circularly polarized π pulses for complete population transfer from the ground state $1s$ to these target states ψ_{nlm} , as well as the conditions for the validity of the theory. Some effects of electron spin are discussed briefly in Sec. VI. The conclusions are presented in Sec. VII.

*Corresponding author. Present address: Institut für Chemie und Biochemie, Freie Universität Berlin, Takustr. 3, 14195 Berlin, Germany. FAX: +49-30-838-54792. Electronic address: barth@chemie.fu-berlin.de

II. RING CURRENTS IN ATOMIC ORBITALS

For the hydrogen atom or one-electron ions He^+ , Li^{2+} , etc. with nuclear charge Z , the atomic orbitals are given in spherical coordinates by [9]

$$\psi_{nlm}(r, \theta, \phi) = C_{nl} e^{-Zr/na_\mu} \left(\frac{2Zr}{na_\mu}\right)^l L_{n-l-1}^{2l+1} \left(\frac{2Zr}{na_\mu}\right) Y_{lm}(\theta, \phi), \quad (1)$$

where C_{nl} is the normalization constant

$$C_{nl} = \sqrt{\left(\frac{2Z}{na_\mu}\right)^3 \frac{(n-l-1)!}{2n(n+l)!}}, \quad (2)$$

a_μ is the Bohr radius for the reduced mass $\mu = m_e M / (m_e + M)$ (m_e and M are respectively the electron and nuclear masses),

$$a_\mu = \frac{4\pi\epsilon_0 \hbar^2}{\mu e^2} \approx a_0, \quad (3)$$

and $L_{n-l-1}^{2l+1}(2Zr/na_\mu)$ and $Y_{lm}(\theta, \phi)$ are the generalized Laguerre polynomial and the spherical harmonic, respectively. The corresponding orbital energy is

$$E_{nlm} = E_n = -\mu c^2 \frac{(Z\alpha)^2}{2n^2}, \quad (4)$$

where $\alpha = e^2 / 4\pi\epsilon_0 \hbar c$ is the fine structure constant. The probability current density in state ψ_{nlm} is

$$\mathbf{j}_{nlm}(r, \theta, \phi) = \frac{i\hbar}{2\mu} (\psi_{nlm} \nabla \psi_{nlm}^* - \psi_{nlm}^* \nabla \psi_{nlm}). \quad (5)$$

Using the Nabla operator in spherical coordinates

$$\nabla = \frac{\partial}{\partial r} \hat{\mathbf{e}}_r + \frac{1}{r} \frac{\partial}{\partial \theta} \hat{\mathbf{e}}_\theta + \frac{1}{r \sin \theta} \frac{\partial}{\partial \phi} \hat{\mathbf{e}}_\phi, \quad (6)$$

one can show that the r and θ components of $\mathbf{j}_{nlm}(r, \theta, \phi)$ vanish. Thus [10,11]

$$\mathbf{j}_{nlm}(r, \theta, \phi) = \frac{\hbar}{\mu r \sin \theta} |\psi_{nlm}|^2 \hat{\mathbf{e}}_\phi \quad (7)$$

has cylindrical symmetry and vanishes for $m=0$. The electric ring current in state ψ_{nlm} is

$$I_{nlm} = -e \int \int \mathbf{j}_{nlm}(r, \theta, \phi) \cdot d\mathbf{S}, \quad (8)$$

where the integral is over the half plane perpendicular to the x/y plane at fixed arbitrary azimuthal angle ϕ with the domains $r=[0, \infty)$ and $\theta=[0, \pi]$. Since $\mathbf{j}_{nlm}(r, \theta, \phi) = \mathbf{0}$ for $m=0$, we also have $I_{nlm}=0$ for $m=0$. For $m \neq 0$, we obtain, inserting Eq. (7) into Eq. (8) and using $d\mathbf{S} = r dr d\theta \hat{\mathbf{e}}_\phi$,

$$I_{nlm} = -e \int_0^\pi \int_0^\infty r \mathbf{j}_{nlm}(r, \theta, \phi) \cdot \hat{\mathbf{e}}_\phi dr d\theta \quad (9)$$

TABLE I. Magnitude of the electric current $|I_{2l\pm 1}|$ [Eq. (14)], the induced magnetic field at the nucleus $|\mathbf{B}_{2l\pm 1}(\mathbf{r}=\mathbf{0})|$ [Eq. (22)], the mean ring current radius $R_{2l\pm 1}$ [Eq. (32)], the transition dipole moment $|\mathbf{M}_{2l\pm 1;100}|$ for transitions between the atomic orbitals $1s$ and $2p_{\pm 1}$ [Eq. (40)], and the lifetime $\tilde{\tau}_{2l\pm 1}$ [Eq. (70)] of electrons occupying $2p_{\pm 1}$ atomic orbitals, depending on the nuclear charges $Z=1, \dots, 13$ using $\mu \approx m_e$ and $a_\mu \approx a_0$.

Atom or ion	Z	$ I_{2l\pm 1} $ (mA)	$ \mathbf{B}_{2l\pm 1}(\mathbf{r}=\mathbf{0}) $ (T)	$R_{2l\pm 1}$ (a_0)	$ \mathbf{M}_{2l\pm 1;100} $ (ea_0)	$\tilde{\tau}_{2l\pm 1}$ (ps)
H	1	0.132	0.52	1.273	0.745	1595.325
He ⁺	2	0.527	4.17	0.637	0.372	99.708
Li ²⁺	3	1.186	14.08	0.424	0.248	19.695
Be ³⁺	4	2.108	33.38	0.318	0.186	6.232
B ⁴⁺	5	3.294	65.19	0.255	0.149	2.553
C ⁵⁺	6	4.744	112.65	0.212	0.124	1.231
N ⁶⁺	7	6.457	178.89	0.182	0.106	0.664
O ⁷⁺	8	8.433	267.03	0.159	0.093	0.389
F ⁸⁺	9	10.674	380.20	0.141	0.083	0.243
Ne ⁹⁺	10	13.177	521.53	0.127	0.074	0.160
Na ¹⁰⁺	11	15.945	694.16	0.116	0.068	0.109
Mg ¹¹⁺	12	18.975	901.21	0.106	0.062	0.077
Al ¹²⁺	13	22.270	1145.81	0.098	0.057	0.056

$$= -\frac{e \hbar m n a_\mu}{\mu 2Z} C_{nl}^2 \int_0^\pi \frac{|Y_{lm}(\theta, \phi)|^2}{\sin \theta} d\theta \int_0^\infty e^{-x} x^{2l} [L_{n-l-1}^{2l+1}(x)]^2 dx. \quad (10)$$

After evaluating the integrals

$$\int_0^\pi \frac{|Y_{lm}(\theta, \phi)|^2}{\sin \theta} d\theta = \frac{2l+1}{4\pi|m|} \quad \text{for } m \neq 0, \quad (11)$$

$$\int_0^\infty e^{-x} x^{2l} [L_{n-l-1}^{2l+1}(x)]^2 dx = \frac{(n+l)!}{(2l+1)(n-l-1)!}, \quad (12)$$

we obtain

$$I_{nlm} = -\text{sgn}(m) \frac{e \hbar Z^2}{2\pi \mu a_\mu^2 n^3}. \quad (13)$$

Thus the magnitudes of the electric ring currents of all degenerate states $(n, l, m \neq 0)$ with the same quantum number n are equal. The direction of the electric ring current is determined by the sign of the quantum number m . The strongest electric current is obtained for $2p_{\pm 1}$ orbitals

$$I_{2l\pm 1} = \mp \frac{e \hbar Z^2}{16\pi \mu a_\mu^2 n^3}. \quad (14)$$

The magnitudes $|I_{2l\pm 1}|$ for $Z=1, \dots, 13$ are listed in Table I.

III. MAGNETIC FIELD INDUCED BY ELECTRIC RING CURRENTS

The magnetic field induced by the electric ring current in the state ψ_{nlm} ($m \neq 0$) is calculated using the Biot-Savart law

$$\mathbf{B}_{nlm}(\mathbf{r}) = -\frac{\mu_0 e}{4\pi} \int_{V'} \frac{\mathbf{j}_{nlm}(\mathbf{r}') \times (\mathbf{r} - \mathbf{r}')}{|\mathbf{r} - \mathbf{r}'|^3} dV'. \quad (15)$$

Using Eq. (7), we obtain

$$\begin{aligned} \mathbf{B}_{nlm}(\mathbf{r}) = & -\frac{\mu_0 e \hbar m}{4\pi\mu} \int_0^\infty dr' r' \int_0^\pi d\theta' |\psi_{nlm}(r', \theta', \phi')|^2 \\ & \times \int_0^{2\pi} d\phi' \{r^2 + r'^2 - 2rr'[\cos\theta \cos\theta' \\ & + \sin\theta \sin\theta' \cos(\phi - \phi')] \}^{-3/2} \{r'[\sin\theta' \cos\theta \\ & - \cos\theta' \sin\theta \cos(\phi - \phi')] \hat{\mathbf{e}}_r + [r \cos(\phi - \phi') \\ & - r' \sin\theta' \sin\theta - r' \cos\theta' \cos\theta \cos(\phi - \phi')] \hat{\mathbf{e}}_\theta \}, \end{aligned} \quad (16)$$

with zero ϕ component. Using the variable transformation $\tilde{\phi} = \phi' - \phi$, we obtain

$$\begin{aligned} \mathbf{B}_{nlm}(\mathbf{r}) = & -\frac{\mu_0 e \hbar m}{4\pi\mu} \int_0^\infty dr' r' \int_0^\pi d\theta' |\psi_{nlm}(r', \theta', \phi')|^2 \\ & \times \int_0^{2\pi} d\tilde{\phi} [r^2 + r'^2 - 2rr'(\cos\theta \cos\theta' \\ & + \sin\theta \sin\theta' \cos\tilde{\phi})]^{-3/2} \times \{r'(\sin\theta' \cos\theta \\ & - \cos\theta' \sin\theta \cos\tilde{\phi}) \hat{\mathbf{e}}_r + [r \cos\tilde{\phi} - r'(\sin\theta' \sin\theta \\ & + \cos\theta' \cos\theta \cos\tilde{\phi})] \hat{\mathbf{e}}_\theta \}, \end{aligned} \quad (17)$$

where the cyclic domain $[0, 2\pi]$ replaces $[-\phi, 2\pi - \phi]$. Thus the induced magnetic field $\mathbf{B}_{nlm}(\mathbf{r})$ is independent of the azimuthal angle ϕ and has cylindrical symmetry. The evaluation of the integral, Eq. (17), is difficult. Here, we focus on the induced magnetic field at the nucleus ($\mathbf{r} = \mathbf{0}$),

$$\begin{aligned} \mathbf{B}_{nlm}(\mathbf{r} = \mathbf{0}) = & -\frac{\mu_0 e \hbar m}{2\mu} \int_0^\infty \frac{dr'}{r'} \int_0^\pi d\theta' \sin\theta' \\ & \times |\psi_{nlm}(r', \theta', \phi')|^2 \hat{\mathbf{e}}_z \\ = & -\frac{\mu_0 e \hbar m}{4\pi\mu} C_{nl}^2 \\ & \times \int_0^\infty dx e^{-x} x^{2l-1} [L_{n-l-1}^{2l+1}(x)]^2 \hat{\mathbf{e}}_z. \end{aligned} \quad (18)$$

Evaluating the integral in Eq. (19), we get

$$\begin{aligned} & \int_0^\infty e^{-x} x^{2l-1} [L_{n-l-1}^{2l+1}(x)]^2 dx \\ & = \frac{n}{l(2l+1)(2l+2)} \frac{(n+l)!}{(n-l-1)!} \quad \text{for } l \geq 1. \end{aligned} \quad (20)$$

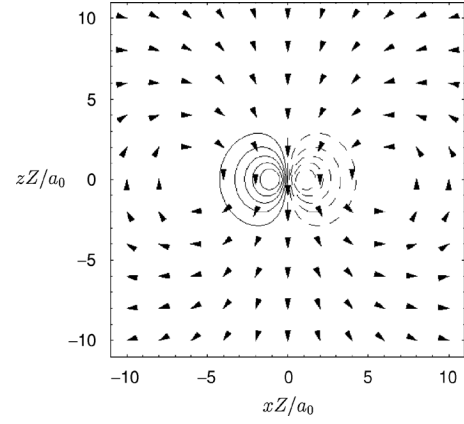


FIG. 1. Toroidal ring current $\mathbf{j}_{2l+1}(\mathbf{r})$ and induced magnetic field $\mathbf{B}_{2l+1}(\mathbf{r})$ of the $2p_{+1}$ orbital, in the x/z plane. The ring current is plotted by means of equicontours for the values $|\mathbf{j}_{2l+1}(x, y = 0, z)| / \max |\mathbf{j}_{2l+1}(\mathbf{r})| = 1/6, 2/6, 3/6, 4/6, 5/6$; cf. Eq. (7); continuous and dashed contour lines indicate toroidal electronic motions toward and away from the reader, respectively. The induced magnetic field is indicated by vectors with length scaled to the maximum value $|\mathbf{B}_{2l+1}(\mathbf{r} = \mathbf{0})|$, Eq. (22). Accordingly, very small values of $|\mathbf{B}_{2l+1}(\mathbf{r})|$ are represented by very short vectors, with lengths smaller than the tops of the arrows. The results apply to arbitrary nuclear charges Z , due to the scalings of the axis, xZ/a_0 and zZ/a_0 .

Inserting Eq. (20) into Eq. (19) yields

$$\mathbf{B}_{nlm}(\mathbf{r} = \mathbf{0}) = -\frac{\mu_0 e \hbar}{\pi \mu a_\mu^3} \frac{Z^3 m}{n^3 l(2l+1)(2l+2)} \hat{\mathbf{e}}_z \quad \text{for } l \geq 1, \quad (21)$$

in accord with the result which is implied by the calculation of the fine structure constant for hydrogenlike atoms, based on the relation between the magnetic field and electronic angular momentum [12]. The largest induced magnetic field $\mathbf{B}_{nlm}(\mathbf{r} = \mathbf{0})$ is obtained for $2p_{\pm 1}$ orbitals,

$$\mathbf{B}_{2l\pm 1}(\mathbf{r} = \mathbf{0}) = \mp \frac{\mu_0 e \hbar Z^3}{96\pi \mu a_\mu^3} \hat{\mathbf{e}}_z, \quad (22)$$

in accord with the strongest electric ring current in $2p_{\pm 1}$ orbitals. Figure 1 shows $\mathbf{j}_{2l+1}(\mathbf{r})$ and $\mathbf{B}_{2l+1}(\mathbf{r})$ for the $2p_{+1}$ orbital. The magnitudes $|\mathbf{B}_{2l\pm 1}(\mathbf{r} = \mathbf{0})|$ depending on Z are also listed in Table I.

IV. RING CURRENT LOOP MODEL

For comparison with the exact result [Eq. (21)], let us also consider the model where the magnetic field is induced by an electron circulating around the nucleus in a current loop [13]

$$\mathbf{B}_{nlm}^{\text{approx}}(\mathbf{r} = \mathbf{0}) = \frac{\mu_0 I_{nlm}}{2 R_{nlm}} \hat{\mathbf{e}}_z. \quad (23)$$

The inverse radius of an electronic orbit circulating around the z axis is $(r \sin\theta)^{-1}$; thus the mean inverse ring current radius R_{nlm}^{-1} in the state ψ_{nlm} with probability current density $\mathbf{j}_{nlm}(r, \theta, \phi)$ is

$$R_{nlm}^{-1} = \langle (r \sin \theta)^{-1} \rangle_j \quad (24)$$

$$= \frac{\int \int (r \sin \theta)^{-1} \mathbf{j}_{nlm}(r, \theta, \phi) \cdot d\mathbf{S}}{\int \int \mathbf{j}_{nlm}(r, \theta, \phi) \cdot d\mathbf{S}} \quad (25)$$

$$= -\frac{e}{I_{nlm}\mu} \int_0^\pi \frac{d\theta}{\sin^2 \theta} \int_0^\infty dr \mathbf{j}_{nlm}(r, \theta, \phi) \hat{\mathbf{e}}_\phi \quad \text{for } m \neq 0, \quad (26)$$

where Eq. (8) and $d\mathbf{S} = r dr d\theta \hat{\mathbf{e}}_\phi$ have been used. (For $m=0$, R_{nlm} is not defined because $\mathbf{j}_{nlm} = \mathbf{0}$.) Inserting Eqs.

(7) and (1) for $\mathbf{j}_{nlm}(r, \theta, \phi)$ and $\psi_{nlm}(r, \theta, \phi)$, respectively, yields

$$R_{nlm}^{-1} = -\frac{e \hbar m}{I_{nlm}\mu} \int_0^\pi \frac{d\theta}{\sin^2 \theta} \int_0^\infty \frac{dr}{r} |\psi_{nlm}(r, \theta, \phi)|^2 \quad (27)$$

$$= -\frac{e \hbar m}{I_{nlm}\mu} C_{nl}^2 \int_0^\pi d\theta \frac{|Y_{lm}(\theta, \phi)|^2}{\sin^2 \theta} \times \int_0^\infty dx e^{-x} x^{2l-1} [L_{n-l-1}^{2l+1}(x)]^2. \quad (28)$$

The first integral is derived from the general formula [14]

$$\int_0^\pi \frac{|Y_{lm}(\theta, \phi)|^2}{\sin^2 \theta} d\theta = \frac{2l+1}{4\pi|m|!} \frac{\Gamma\left(|m| - \frac{1}{2}\right) \Gamma\left(l + \frac{1}{2}\right)}{(l-1)!} {}_4F_3 \left(\begin{matrix} \frac{3}{2}, & -\frac{1}{2}, & -\frac{1}{2}(l-|m|-1), & -\frac{1}{2}(l-|m|) \\ 1, & \frac{1}{2}-l, & |m|+1 & \end{matrix} ; 1 \right), \quad (29)$$

where Γ and ${}_4F_3$ are the Euler gamma function and the generalized hypergeometric function, respectively. The second integral is given by Eq. (20). Thus the mean ring current radius is

$$R_{nlm} = \frac{l(2l+2)(l-1)! (|m|-1)!}{2Z\Gamma\left(l + \frac{1}{2}\right)\Gamma\left(|m| - \frac{1}{2}\right)} a_\mu {}_4F_3 \left(\begin{matrix} \frac{3}{2}, & -\frac{1}{2}, & -\frac{1}{2}(l-|m|-1), & -\frac{1}{2}(l-|m|) \\ 1, & \frac{1}{2}-l, & |m|+1 & \end{matrix} ; 1 \right)^{-1} \quad \text{for } m \neq 0. \quad (30)$$

Thus R_{nlm} depends on l , $|m|$, and Z but not on n . For the special cases $l=|m| \geq 1$ and $l=|m|+1 \geq 2$, the function ${}_4F_3(\dots)$ is equal to 1; thus

$$R_{nlm} = \frac{l(2l+2)(l-1)! (|m|-1)!}{2Z\Gamma\left(l + \frac{1}{2}\right)\Gamma\left(|m| - \frac{1}{2}\right)} a_\mu \quad \text{for } l=|m| \geq 1 \quad \text{and} \quad l=|m|+1 \geq 2. \quad (31)$$

In particular, the mean ring current radius of an electron in the $2p_{\pm 1}$ orbital with maximum ring current and strongest induced magnetic field is

$$R_{21\pm 1} = \frac{4a_\mu}{\pi Z}. \quad (32)$$

The values of $R_{21\pm 1}$ for $Z=1, \dots, 13$ are also listed in Table I. Inserting the results I_{nlm} [Eq. (13)] and R_{nlm} [Eq. (31)] into Eq. (23) gives

$$\mathbf{B}_{nlm}^{\text{approx}}(\mathbf{r} = \mathbf{0}) = -\frac{\mu_0 e \hbar Z^3 m}{\pi \mu a_\mu^3 n^3 |m|!} \frac{\Gamma\left(l + \frac{1}{2}\right) \Gamma\left(|m| - \frac{1}{2}\right)}{2l(2l+2)(l-1)!} \hat{\mathbf{e}}_z \quad \text{for } l=|m| \geq 1 \quad \text{and} \quad l=|m|+1 \geq 2. \quad (33)$$

Accordingly, the ratio of the approximate to the exact induced magnetic fields at the nucleus ($\mathbf{r} = \mathbf{0}$) is

$$\frac{\mathbf{B}_{nlm}^{\text{approx}}(\mathbf{r} = \mathbf{0})}{\mathbf{B}_{nlm}(\mathbf{r} = \mathbf{0})} = \frac{(2l+1)\Gamma\left(l + \frac{1}{2}\right)\Gamma\left(l - \frac{1}{2}\right)}{2(l-1)! l!} \quad \text{for } l=|m| \geq 1 \quad (34)$$

$$= \frac{(2l+1)\Gamma\left(l + \frac{1}{2}\right)\Gamma\left(l - \frac{3}{2}\right)}{2(l-1)!^2} \quad \text{for } l=|m|+1 \geq 2. \quad (35)$$

Applications of these formulas show that the ratio for $l=|m|$ is smaller than the one for $l=|m|+1$ because $\psi_{nl\pm(l-1)}$ is more appropriately represented by two separate ring current loops, rather than a single ring current for $\psi_{nl\pm l}$. By extrapolation, the model of the single current loop is inadequate for $l > |m|$. For $l=|m|$, the values of the ratio [Eq. (34)] are 2.36 for $np_{\pm 1}$ orbitals, 1.47 for $nd_{\pm 2}$ orbitals, 1.29 for $nf_{\pm 3}$ orbitals, etc. One can show that the ratio [Eq. (34)] converges to 1 for $l=|m| \rightarrow \infty$. This supports the ring current loop model, which in turn confirms the results of Secs. II and III.

**V. CIRCULARLY POLARIZED π PULSES
FOR COMPLETE POPULATION TRANSFER
FROM $1s$ TO $2p_{\pm 1}$ ATOMIC ORBITALS**

Now let us design laser pulses, which excite an electron from the ground state $1s$ to the target atomic orbital $2p_{\pm 1}$, representing the strongest electric ring currents and induced magnetic fields. For this purpose, previous work [4,5] suggests that we employ right (+) or left (−) circularly polarized π laser pulses propagating along the z direction, whose electric field is given by

$$\mathcal{E}_{\pm}(t) = \mathcal{E}_0 \sin^2\left(\frac{\pi t}{t_p}\right) [\cos(\omega t) \hat{\mathbf{e}}_x \pm \sin(\omega t) \hat{\mathbf{e}}_y], \quad (36)$$

where the maximum amplitude is \mathcal{E}_0 , the resonant frequency is

$$\omega = \omega_{21\pm 1;100} = \frac{3}{8} \frac{\mu c^2}{\hbar} (Z\alpha)^2, \quad (37)$$

and the total pulse duration t_p satisfies

$$\frac{|\mathbf{M}_{21\pm 1;100}| \mathcal{E}_0 t_p}{\sqrt{2} \hbar} = \pi. \quad (38)$$

Here, $\mathbf{M}_{21\pm 1;100}$ is the $\psi_{100} \rightarrow \psi_{21\pm 1}$ transition dipole element, given by

$$\begin{aligned} \mathbf{M}_{21\pm 1;100} &= -e \int \int \int \psi_{21\pm 1}^* \begin{pmatrix} x \\ y \\ z \end{pmatrix} \psi_{100} dV \\ &= -\frac{128}{243} \frac{ea\mu}{Z} \begin{pmatrix} 1 \\ \mp i \\ 0 \end{pmatrix}, \end{aligned} \quad (39)$$

thus

$$|\mathbf{M}_{21\pm 1;100}| = \sqrt{2} \frac{128}{243} \frac{ea\mu}{Z}. \quad (40)$$

The magnitudes $|\mathbf{M}_{21\pm 1;100}|$ depending on Z are also listed in Table I. The corresponding laser field intensity is

$$\mathcal{I}(t) = \varepsilon_0 c |\mathcal{E}_{\pm}(t)|^2 = \varepsilon_0 c \mathcal{E}_0^2 \sin^4\left(\frac{\pi t}{t_p}\right). \quad (41)$$

The laser-driven electronic wave packet is obtained by solving the Schrödinger equation

$$i \hbar \frac{d}{dt} \psi_{\pm}(t) = H(t) \psi_{\pm}(t) = \left[-\frac{\hbar^2}{2\mu} \Delta - \frac{Ze^2}{4\pi\varepsilon_0 r} + e\mathbf{r} \cdot \mathcal{E}_{\pm}(t) \right] \psi_{\pm}(t) \quad (42)$$

with semiclassical dipole approximation, for the initial condition

$$\psi_{\pm}(t=0) = \psi_{100}. \quad (43)$$

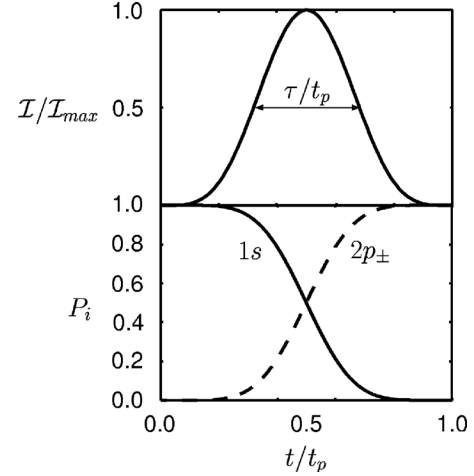


FIG. 2. Complete population transfer from the ground ($1s$) to the excited target atomic orbitals ($2p_+$ or $2p_-$) with strongest electric ring currents and magnetic fields, induced by right (+) or left (−) circularly polarized π laser pulses with intensity $\mathcal{I}(t)$ and total duration t_p [cf. Eqs. (36)–(41), (48), and (49), and the scalings, Eqs. (50)–(56)]. The corresponding laser parameters for $Z=1, \dots, 13$ are given in Table II.

The target state is

$$\psi_{\pm}(t > t_p) = \psi_{21\pm 1} e^{-i(\omega_{21\pm 1;100} t + \eta)}, \quad (44)$$

where η is an irrelevant phase. The solution of Eq. (42) corresponding to right (+) or left (−) circularly polarized π pulses, Eqs. (36)–(41), is given approximately by the simple two-state expansion

$$\psi_{\pm}(t) \approx C_{1s}(t) e^{-iE_1 t/\hbar} \psi_{100} + C_{2p_{\pm 1}}(t) e^{-iE_2 t/\hbar} \psi_{21\pm 1}, \quad (45)$$

where the coefficients for the $1s$ and $2p_{\pm 1}$ components are

$$C_{1s}(t) = \cos \left[\frac{|\mathbf{M}_{21\pm 1;100}| \mathcal{E}_0}{\sqrt{2} \hbar} \int_0^t \sin^2\left(\frac{\pi t'}{t_p}\right) dt' \right], \quad (46)$$

$$C_{2p_{\pm 1}}(t) = -i \sin \left[\frac{|\mathbf{M}_{21\pm 1;100}| \mathcal{E}_0}{\sqrt{2} \hbar} \int_0^t \sin^2\left(\frac{\pi t'}{t_p}\right) dt' \right], \quad (47)$$

respectively. The corresponding populations of the $1s$ and $2p_{\pm 1}$ orbitals, given by

$$P_{1s}(t) = |C_{1s}(t)|^2 = \cos^2 \left[\frac{|\mathbf{M}_{21\pm 1;100}| \mathcal{E}_0}{\sqrt{2} \hbar} \int_0^t \sin^2\left(\frac{\pi t'}{t_p}\right) dt' \right], \quad (48)$$

$$P_{2p_{\pm 1}}(t) = |C_{2p_{\pm 1}}(t)|^2 = \sin^2 \left[\frac{|\mathbf{M}_{21\pm 1;100}| \mathcal{E}_0}{\sqrt{2} \hbar} \int_0^t \sin^2\left(\frac{\pi t'}{t_p}\right) dt' \right], \quad (49)$$

are plotted in Fig. 2, together with the laser intensity $\mathcal{I}(t)$. Note that the solution, Eqs. (45)–(47), of Eq. (42) for H ($Z=1$) yields equivalent solutions for arbitrary values of Z , using the scalings

TABLE II. Laser parameters of the circularly polarized π pulses [Eq. (36)] for total population transfer from $1s$ to $2p_{\pm}$ atomic orbitals for $Z=1, \dots, 13$, for two cases of the spectral width parameter $\gamma=0.1$ and $\gamma=0.01$ [Eq. (57)], and the corresponding total number of laser cycles $N_{\text{cyc}} \approx 78$ and $N_{\text{cyc}} \approx 778$ [Eqs. (60) and (61)], respectively. The parameters $\omega = \omega_{21\pm 1;100}$, $\tau \approx 0.364t_p$, \mathcal{E}_0 , and \mathcal{I}_{max} denote the resonant frequency [Eq. (37)], the duration [Eq. (58)], the field strength [Eq. (62)], and the maximum intensity [Eq. (63)], respectively. Entries denoted “-” are in the relativistic regime [Eq. (64)].

Atom or ion	Z	$\gamma=0.1, N_{\text{cyc}} \approx 78$				$\gamma=0.01, N_{\text{cyc}} \approx 778$		
		$\hbar\omega$ (eV)	τ (fs)	\mathcal{E}_0 (V m ⁻¹)	\mathcal{I}_{max} (W cm ⁻²)	τ (fs)	\mathcal{E}_0 (V m ⁻¹)	\mathcal{I}_{max} (W cm ⁻²)
H	1	10.2	11.48	2.35×10^9	1.47×10^{12}	114.8	2.35×10^8	1.47×10^{10}
He ⁺	2	40.8	2.869	1.88×10^{10}	9.40×10^{13}	28.69	1.88×10^9	9.40×10^{11}
Li ²⁺	3	91.8	1.275	6.35×10^{10}	1.07×10^{15}	12.75	6.35×10^9	1.07×10^{13}
Be ³⁺	4	163.3	0.717	1.51×10^{11}	6.02×10^{15}	7.173	1.51×10^{10}	6.02×10^{13}
B ⁴⁺	5	255.1	0.459	2.94×10^{11}	2.30×10^{16}	4.591	2.94×10^{10}	2.30×10^{14}
C ⁵⁺	6	367.4	0.319	5.08×10^{11}	6.86×10^{16}	3.188	5.08×10^{10}	6.86×10^{14}
N ⁶⁺	7	500.0	0.234	8.07×10^{11}	1.73×10^{17}	2.342	8.07×10^{10}	1.73×10^{15}
O ⁷⁺	8	653.1	0.179	1.21×10^{12}	3.85×10^{17}	1.793	1.21×10^{11}	3.85×10^{15}
F ⁸⁺	9	826.5	0.142	1.72×10^{12}	7.81×10^{17}	1.417	1.72×10^{11}	7.81×10^{15}
Ne ⁹⁺	10	1020.4	-	-	-	1.148	2.35×10^{11}	1.47×10^{16}
Na ¹⁰⁺	11	1234.7	-	-	-	0.949	3.13×10^{11}	2.60×10^{16}
Mg ¹¹⁺	12	1469.4	-	-	-	0.797	4.07×10^{11}	4.39×10^{16}
Al ¹²⁺	13	1724.5	-	-	-	0.679	5.17×10^{11}	7.09×10^{16}

$$\mathbf{r} \rightarrow \mathbf{r}/Z, \quad (50)$$

$$\mathbf{p} = -i\hbar \nabla \rightarrow \mathbf{p}Z, \quad (51)$$

$$\mathcal{E}_0 \rightarrow \mathcal{E}_0 Z^3, \quad (52)$$

$$\mathcal{I}_{\text{max}} = \varepsilon_0 c \mathcal{E}_0^2 \rightarrow \mathcal{I}_{\text{max}} Z^6, \quad (53)$$

$$\omega = \omega_{21\pm 1;100} \rightarrow \omega Z^2, \quad (54)$$

$$t \rightarrow t/Z^2, \quad (55)$$

$$t_p \rightarrow t_p/Z^2. \quad (56)$$

The corresponding optimal laser parameters for total population transfer from $1s$ to $2p_{\pm 1}$ orbitals for $Z=1, \dots, 13$ are given in Table II.

The validity of the results, Eqs. (36)–(49), depends on the following various conditions.

(i) In order to avoid competing transitions from the ground state to other excited states, e.g., $3p_{\pm 1}$, the spectral width of the laser pulse Γ should be smaller than the energy gap between the excited states $2p_{\pm 1}$ and $3p_{\pm 1}$. Thus the condition for the spectral width is

$$\Gamma = \gamma(E_3 - E_2) = \gamma \frac{5}{72} \mu c^2 (Z\alpha)^2 \approx \gamma 1.89 \text{ eV} Z^2, \quad \gamma \ll 1, \quad (57)$$

where the spectral width parameter γ should be sufficiently small, say, $\gamma \leq 0.1$.

(ii) For the chosen \sin^2 envelope, Eq. (36), the corresponding mean pulse duration (see Fig. 2)

$$\tau \approx 0.364t_p \quad (58)$$

is related to Γ by [1]

$$\tau \approx \frac{3.295\hbar}{\Gamma} \approx \frac{1}{\gamma} 47.45 \frac{\hbar}{\mu c^2 (Z\alpha)^2} \approx \frac{1}{\gamma} 1.148 \text{ fs} \frac{1}{Z^2}, \quad \gamma \ll 1, \quad (59)$$

i.e., τ should be sufficiently long. We note in passing that the corresponding total number of laser cycles N_{cyc} also depends on the spectral width parameter γ , but not on Z ,

$$N_{\text{cyc}} = \frac{\omega_{100;21\pm 1} t_p}{2\pi} \approx \frac{1}{\gamma} 7.780, \quad \gamma \ll 1. \quad (60)$$

For example,

$$N_{\text{cyc}} \approx 78 \text{ for } \gamma=0.1, \quad N_{\text{cyc}} \approx 778 \text{ for } \gamma=0.01. \quad (61)$$

(iii) The condition for the circularly polarized π pulse [Eq. (38)] implies that the maximum amplitude

$$\mathcal{E}_0 = \frac{\pi\hbar}{Mt_p} = \frac{243\pi\hbar Z}{128ea_{\mu} t_p} \approx \gamma 23.53 \text{ GV m}^{-1} Z^3, \quad \gamma \ll 1 \quad (62)$$

and also the corresponding maximum intensity \mathcal{I}_{max}

$$\mathcal{I}_{\text{max}} = \varepsilon_0 c \mathcal{E}_0^2 \approx \gamma^2 147.0 \text{ TW cm}^{-2} Z^6, \quad \gamma \ll 1 \quad (63)$$

depend on the spectral width parameter γ and on the nuclear charge Z . Now, we require that the laser pulse be in the nonrelativistic regime, i.e.,

$$\mathcal{I}_{\max} \leq 10^{18} \text{ W cm}^{-2}. \quad (64)$$

This condition implies a restriction on the maximum value of Z , depending on the spectral width parameter γ . For example,

$$Z \leq 9 \text{ for } \gamma = 0.1, \quad Z \leq 20 \text{ for } \gamma = 0.01. \quad (65)$$

(iv) Still another upper limit of the nuclear charge Z is imposed by the requirement that, for the present nonrelativistic theory, the electron should have nonrelativistic velocity, say, $v \leq c/10$. Using the virial theorem

$$\langle T_{\text{kin}} \rangle \equiv \frac{\mu v_n^2}{2} = -E_n = \mu c^2 \frac{(Z\alpha)^2}{2n^2}, \quad (66)$$

v_n can be estimated as

$$v_n = \frac{Z\alpha c}{n}. \quad (67)$$

The requirement $v_n \leq c/10$ then implies that

$$Z(n=1) \leq \frac{1}{10\alpha} \approx 13. \quad (68)$$

Evidently, the conditions [Eqs. (65) and (68)] imply the restrictions $Z \leq 9$ for $\gamma = 0.1$ or $Z \leq 13$ for $\gamma = 0.01$.

(v) The total pulse duration t_p must be much smaller (say, by a factor 0.1) than the lifetime of the excited state $\tilde{\tau}_{21\pm 1}$, i.e.,

$$t_p \leq \frac{1}{10} \tilde{\tau}_{21\pm 1}, \quad (69)$$

where [13]

$$\tilde{\tau}_{21\pm 1} \approx \frac{3\pi\epsilon_0 c^3 \hbar}{\omega_{21\pm 1;100}^3} \frac{1}{|\mathbf{M}_{21\pm 1;100}|^2} \approx \frac{6561\pi\epsilon_0 c^3 \mu^3 a_0^4}{64\hbar^2 e^2 Z^4}, \quad (70)$$

see Table I. The condition [Eq. (69)] implies another restriction of the nuclear charge Z depending on the spectral width parameter γ [cf. Eqs. (58) and (59)], namely,

$$3.153 \text{ fs} \frac{1}{\gamma Z^2} \leq 159.5 \text{ ps} \frac{1}{Z^4}. \quad (71)$$

For example, this condition [Eq. (71)] calls for

$$Z \leq 71 \text{ for } \gamma = 0.1, \quad Z \leq 22 \text{ for } \gamma = 0.01. \quad (72)$$

Comparison with the previous limits, Eqs. (65) and (68), shows that the restriction [Eq. (72)] is satisfied already.

(vi) The laser intensities have to be sufficiently weak to avoid competing ionization. The ionization probability P_{ion} , which depends on the electric field \mathcal{E}_0 , is estimated as [15,16]

$$P_{\text{ion}} = 4\omega_a Z^5 \frac{\mathcal{E}_a}{\mathcal{E}_0} \exp\left(-\frac{2Z^3 \mathcal{E}_a}{3 \mathcal{E}_0}\right), \quad (73)$$

where $\omega_a = \hbar / (m_e a_0^2) \approx 4.134 \times 10^{16} \text{ s}^{-1}$ and $\mathcal{E}_a = \hbar^2 / (em_e a_0^3) \approx 514.221 \text{ GV m}^{-1}$ are atomic units of frequency and elec-

tric field, respectively. Using the expression [Eq. (62)] for the electric field, we estimate ionization probabilities of

$$P_{\text{ion}} \approx 1.926 \times 10^{-44} Z^2 \text{ s}^{-1} \text{ for } \gamma = 0.1, \quad (74)$$

$$P_{\text{ion}} \approx 6.676 \times 10^{-613} Z^2 \text{ s}^{-1} \text{ for } \gamma = 0.01.$$

Accordingly, the ionization probability can be neglected for all known values of nuclear charges Z .

In conclusion, the two-state solution [Eq. (45)] of the time-dependent Schrödinger equation is supported by all conditions (i)–(vi), subject to the “nonrelativistic” restrictions, Eqs. (65) and (68).

VI. ROLE OF ELECTRON SPIN

Finally, it will be shown that the previous results for atomic orbitals ψ_{nlm} apply also to spin orbitals $\psi_{nlm_p m_s}$, with corresponding relativistic modification of the transition frequency. In fact, the Dirac equation yields corresponding approximate representations $\tilde{\psi}_{nlj m_j}$ of the exact wave functions with quantum numbers $s=1/2$, $j=l\pm s$, $m_j=-j, \dots, j$, with relativistic energies [17]

$$E_{nj} = \mu c^2 \left\{ 1 + \left[\frac{Z\alpha}{n - (j + \frac{1}{2}) + \sqrt{(j + \frac{1}{2})^2 - (Z\alpha)^2}} \right]^2 \right\}^{-1/2} \quad (75)$$

$$= \mu c^2 \left[1 - \frac{(Z\alpha)^2}{2n^2} - \frac{(Z\alpha)^4}{2n^3} \left(\frac{1}{j + 1/2} - \frac{3}{4n} \right) + O((Z\alpha)^6) \right], \quad (76)$$

in particular,

$$E_{1(1/2)} \approx \mu c^2 + E_1 - \frac{1}{8} \mu c^2 (Z\alpha)^4, \quad (77)$$

$$E_{2(1/2)} \approx \mu c^2 + E_2 - \frac{5}{128} \mu c^2 (Z\alpha)^4, \quad (78)$$

$$E_{2(3/2)} \approx \mu c^2 + E_2 - \frac{1}{128} \mu c^2 (Z\alpha)^4. \quad (79)$$

The wave functions $\tilde{\psi}_{nlj m_j}$ ($n=1,2$) may be expressed in terms of the previous atomic orbitals ψ_{nlm} or corresponding spin orbitals $\psi_{nlm_p m_s}$ [18]

$$\tilde{\psi}_{10(1/2)\pm 1/2} \approx \psi_{100\pm 1/2}, \quad (80)$$

$$\tilde{\psi}_{21(1/2)\pm 1/2} \approx \mp \sqrt{\frac{1}{3}} \psi_{210\pm 1/2} \pm \sqrt{\frac{2}{3}} \psi_{21\pm 1\mp 1/2}, \quad (81)$$

$$\tilde{\psi}_{21(3/2)\pm 1/2} \approx \sqrt{\frac{2}{3}} \psi_{210\pm 1/2} + \sqrt{\frac{1}{3}} \psi_{21\pm 1\mp 1/2}, \quad (82)$$

$$\tilde{\psi}_{21(3/2)\pm 3/2} \approx \psi_{21\pm 1\pm 1/2}. \quad (83)$$

Accordingly, the spin orbitals $\psi_{100\pm 1/2}$ and $\psi_{21\pm 1\pm 1/2}$, which represent the previous atomic orbitals $1s$ and $2p_{\pm 1}$ multiplied

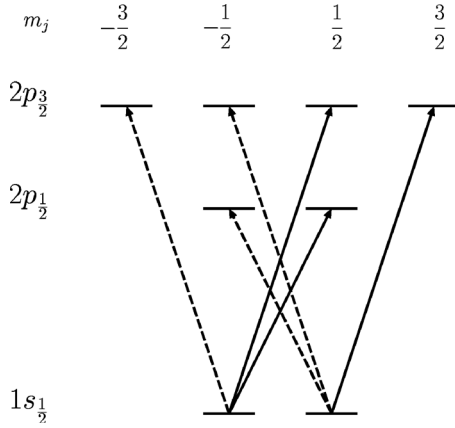


FIG. 3. Schematic representation of dipole allowed transitions from the ground $1s_{1/2}$ to excited $2p_{1/2}$, $2p_{3/2}$, $2p_{3/2}$, and $2p_{3/2}$ states induced by right (+) (solid lines) or left (-) (dashed lines) circularly polarized laser pulses.

by spin functions (α for $m_s=1/2$ and β for $m_s=-1/2$), i.e., $1s\alpha$, $1s\beta$ and $2p_{+1}\alpha$, $2p_{-1}\beta$, are excellent approximations to $\tilde{\psi}_{10(1/2)\pm 1/2}$ and $\tilde{\psi}_{21(3/2)\pm 3/2}$, respectively. The transitions, which can be induced by right (+) or left (-) circularly polarized laser pulse, are illustrated in Fig. 3. Hence the previous results for right or left circularly polarized π pulses for transitions $1s \rightarrow 2p_{+1}$ or $1s \rightarrow 2p_{-1}$ are also valid, approximately, for the corresponding transitions $1s_{(1/2)(1/2)} \rightarrow 2p_{(3/2)(3/2)}$ or $1s_{1/2-1/2} \rightarrow 2p_{3/2-3/2}$, respectively. The resonance condition [Eq. (37)] then has to be replaced, however, by

$$\hbar\omega = E_{2(3/2)} - E_{1(1/2)} \approx \frac{3}{8}\mu c^2(Z\alpha)^2 + \frac{15}{128}\mu c^2(Z\alpha)^4. \quad (84)$$

VII. DISCUSSION AND CONCLUSIONS

The present derivation of the closed form expressions for electric ring currents I_{nlm} [Eq. (13)] and corresponding magnetic fields $\mathbf{B}_{nlm}(\mathbf{r}=\mathbf{0})$ [Eq. (21)] induced by electrons in hydrogenlike atomic orbitals ψ_{nlm} yields maximum values for electrons occupying $2p_{\pm 1}$ orbitals [cf. Eqs. (14) and (22), respectively]. The corresponding values given in Table I predict that the effects should increase dramatically with nuclear charge Z , e.g., the magnitudes of the ring current $I_{21\pm 1}$ and magnetic field $\mathbf{B}_{21\pm 1}(\mathbf{r}=\mathbf{0})$ should increase from the modest values of 0.133 mA and 0.52 T for H ($Z=1$), by two or even three orders of magnitude, to the values of 22.3 mA and 1146 T for Al^{12+} ($Z=13$). This systematic trend can be understood as a consequence of the scalings, Eqs. (50)–(56), which imply the corresponding scalings for the electric ring currents $I_{nlm} \propto Z^2$, Eq. (13), and the induced magnetic fields $\mathbf{B}_{nlm}(\mathbf{r}=\mathbf{0}) \propto Z^3$, Eq. (21). We note in passing that the same scalings are also in accord with the fact that various other properties do not depend on Z , including the mean angular momenta $\sqrt{l(l+1)}\hbar$, or their z components $m\hbar$, as well as the magnetic dipole moments [13]

$$\mu_e = -m_j\mu_B \left[1 + \frac{j(j+1) + s(s+1) - l(l+1)}{2j(j+1)} \right], \quad (85)$$

where $\mu_B = e\hbar/2m_e$ is the Bohr magneton and $s=1/2$, $j=l\pm s$, and $m_j=-j, \dots, j$. For the special cases of electrons in atomic orbitals $\psi_{nl\pm l}$, the trends for $I_{nl\pm l}$ and $\mathbf{B}_{nl\pm l}(\mathbf{r}=\mathbf{0})$ can also be rationalized by means of the electric ring current loop model (cf. Sec. IV), as follows: Atomic orbitals $\psi_{nl\pm l}$ have z components of angular momentum $m\hbar=l\hbar$, irrespective of the nuclear charge Z . For increasing values of Z , the corresponding mean radii of the electronic flux densities $R_{nl\pm l}$ decrease as $1/Z$ [cf. Eq. (31)]. As a consequence, the corresponding mean momenta or velocities along the current loops increase as Z ; hence the frequencies of cyclic electronic orbits along the perimeters $2\pi R_{nl\pm l}$ increase as Z^2 and, therefore, also the corresponding electric ring currents $I_{nl\pm l}$ increase as Z^2 . The expression, Eq. (23), for the magnetic field induced by the ring current then implies that the resulting magnetic field should, indeed, increase as Z^3 .

We have designed circularly polarized π laser pulses for selective preparation of these $2p_{\pm 1}$ target states, inducing complete population transfer $1s \rightarrow 2p_{\pm 1}$ [cf. Eq. (36) and Fig. 2]. The laser parameters vary strongly depending on the nuclear charge Z [cf. the scaling relations, Eqs. (50)–(56)], and on the spectral width parameter γ [cf. Eq. (57) and Table II]. Note that the strongest pulses considered ($\mathcal{I}_{\max} = 10^{18} \text{ W cm}^{-2}$) have rather large maximum values of magnetic laser field ($\sim 6500 \text{ T}$), but these are switched off after the pulse, whereas the induced strong magnetic fields survive during the lifetime of the excited states. The derivation of these pulses is based on a simple two-state approximation for the laser-driven hydrogenlike atom [cf. Eq. (45)]. The validity of this approximation is supported by six criteria [(i)–(vi)], discussed in Sec. V.

The reliability of the two-state model, as presented in Sec. V, may be verified by means of numerical simulations. Accurate methods for this purpose have been developed only rather recently, and they are quite demanding; cf. Refs. [19–21]. The advantage of the numerical simulations is that they allow one to extend the present approach to domains beyond the validity of the criteria (i), (ii), and (vi). For example, they could be employed to simulate excitations of electric ring currents and induced magnetic fields in atomic orbitals by means of ultrashort few-cycle laser pulses. Our previous experience with quantum simulations of these phenomena in molecules [1–5] suggests that the present π pulses would still be useful as a reference for designing reoptimized π laser pulses. Additional challenges include extensions to the relativistic regime, and to simulations of laser-driven electron circulation represented in terms of time-dependent hybrid orbitals; cf. Refs. [1–3].

The present phenomenon should have applications beyond the H atom and analogous one-electron ions to more complicated multielectron systems including atoms, ions (see Refs. [22,23]), and even molecules or molecular ions. For example, circularly polarized laser pulses can excite electron circulations or ring currents and related magnetic fields in oriented molecules [1–5]. These may be expressed approximately in terms of linear combinations of atomic orbitals–

molecular orbitals (LCAO-MO), and the results of the present analysis of single atomic orbitals (AOs) may hence be carried over to LCAO-MOs. In favorable situations (e.g., in cases where the excited state is well described as a single dominant symmetry-adapted Slater determinant representing the excitation of a single electron to a MO, which consists of only a few AOs), the present results for the AOs can be used directly to estimate the magnetic fields at the nuclei of the excited molecule. As an example, consider the excitation of the toroidal ring current around the molecular bond of the oriented AlCl molecule, which has served as a motivation for the present study (see Sec. I). Here, the right (+) or left (−) circularly polarized laser pulses essentially excite the ground $X^1\Sigma^+$ to the degenerate $A^1\Pi_+$ or $A^1\Pi_-$ states, which can be described approximately as a single symmetry-adapted Slater determinant with the dominant (84%) transition from the highest occupied molecular orbital (HOMO) 9σ to the degenerate lowest unoccupied molecular orbital (LUMO) $4\pi_+$ or $4\pi_-$, respectively [5]. The latter have dominant LCAO-MO expansions $4\pi_\pm \approx c_{3p_\pm(\text{Al})}3p_\pm(\text{Al}) + c_{3p_\pm(\text{Cl})}3p_\pm(\text{Cl})$ with the coefficients $|c_{3p_\pm(\text{Al})}|^2 \approx 0.9$ and $|c_{3p_\pm(\text{Cl})}|^2 \approx 0.1$. For example, using simple Slater rules [24,25], we estimate the effective nuclear charge for the Al atom to be $Z_{\text{eff}} = 13 - 2 - 8 \times 0.85 - 2 \times 0.35 = 3.5$, and the corresponding magnetic field induced at the Al nucleus, according to Eq. (21), to be $|\mathbf{B}_{31\pm}(\mathbf{r}=\mathbf{R}_{\text{Al}})| = 6.0$ T. The semiquantitative agreement with the accurate result based on *ab initio* quantum chemistry [5], $|\mathbf{B}(\mathbf{r}=\mathbf{R}_{\text{Al}})| = 7.7$ T, allows an illuminating interpretation of the underlying mechanism: In essence the magnetic field of the AlCl molecule is due to a single electron occupying the given LCAO-MO $4\pi_\pm$ orbital,

with the properties of the AOs as derived in the present paper. Indeed, this example suggests additional applications such as enhancement of nuclear magnetic resonance due to the magnetic fields induced by ultrashort circularly polarized laser pulses replacing the magnetic field in the laboratory [26] and monitoring the electronic ring currents, e.g., by means of state selective spectra of high harmonic generation; see also Refs. [27,28].

ACKNOWLEDGMENTS

Encouraging discussions with Professor A. F. Starace (University of Nebraska), Dr. St. Chelkowski (Université de Sherbrooke), and Professor A. D. Bandrauk (Université de Sherbrooke) during the Attosecond Science Workshop held at the Kavli Institute of Theoretical Physics (KITP) of the University of California at Santa Barbara (UCSB) are gratefully acknowledged. We are also grateful to Professor L. Serrano-Andrés (Universitat de València) for allowing us to refer to the stimulating results [5] prior to publication, to Professor G. Buntkowsky (Universität Jena) for suggesting applications of nuclear magnetic resonance induced by the laser-driven magnetic fields of electrons in molecular orbitals, and to Professor D. J. Diestler (University of Nebraska) for his advice while preparing the manuscript. We also thank Deutsche Forschungsgemeinschaft (DFG, project Ma 515/23-1) and Fonds der Chemischen Industrie for financial support. This research was also supported in part at KITP by the National Science Foundation under Grant No. PHY99-07949.

-
- [1] I. Barth and J. Manz, *Angew. Chem., Int. Ed.* **45**, 2962 (2006).
 [2] I. Barth and J. Manz, in *Femtochemistry VII: Fundamental Ultrafast Processes in Chemistry, Physics, and Biology*, edited by A. W. Castleman, Jr. and M. L. Kimble (Elsevier, Amsterdam, 2006), pp. 441–454.
 [3] I. Barth, L. González, C. Lasser, J. Manz, and T. Rozgonyi, in *Coherent Control of Molecules*, edited by B. Lasorne and G. A. Worth (CCP6, Daresbury, 2006), pp. 18–27.
 [4] I. Barth, J. Manz, Y. Shigeta, and K. Yagi, *J. Am. Chem. Soc.* **128**, 7043 (2006).
 [5] I. Barth, J. Manz, and L. Serrano-Andrés (to be published).
 [6] J. Jusélius and D. Sundholm, *J. Org. Chem.* **65**, 5233 (2000).
 [7] E. Steiner, A. Soncini, and P. W. Fowler, *Org. Biomol. Chem.* **3**, 4053 (2005).
 [8] A. F. Starace (University of Nebraska) and St. Chelkowski (Université de Sherbrooke) (private communication), Attosecond Science Workshop, Kavli Institute of Theoretical Physics (KITP) of the University of California at Santa Barbara (UCSB), <http://www.kitp.ucsb.edu>.
 [9] P. A. Tipler and R. A. Llewellyn, *Modern Physics* (W. H. Freeman and Company, New York, 2003).
 [10] P. Bronner, Diploma thesis, Universität Karlsruhe, <http://www.hydrogenlab.de>, 2004.
 [11] W. Greiner, *Theoretische Physik, Bd. 4: Quantenmechanik: Einführung* (Verlag Harri Deutsch, Frankfurt am Main, 2005).
 [12] H. Haken and H. C. Wolf, *Atom- und Quantenphysik* (Springer-Verlag, Berlin, 1993).
 [13] A. Hinchliffe and R. W. Munn, *Molecular Electromagnetism* (John Wiley and Sons Ltd., Chichester, 1985).
 [14] M. A. Rashid, *J. Phys. A* **19**, 2505 (1986).
 [15] P. B. Corkum, N. H. Burnett, and F. Brunel, *Phys. Rev. Lett.* **62**, 1259 (1989).
 [16] A. D. Bandrauk, E. S. Sedik, and C. F. Matta, *J. Chem. Phys.* **121**, 7764 (2004).
 [17] F. Schwabl, *Quantenmechanik für Fortgeschrittene* (Springer-Verlag, Berlin, 1997).
 [18] C. Cohen-Tannoudji, B. Diu, and F. Laloë, *Quantum Mechanics* (John Wiley and Sons Ltd., New York, 1977).
 [19] A. D. Bandrauk and H. Z. Lu, *J. Mol. Struct.* **547**, 97 (2001).
 [20] B. I. Schneider, L. A. Collins, and S. X. Hu, *Phys. Rev. E* **73**, 036708 (2006).
 [21] S. X. Hu and L. A. Collins, *Phys. Rev. A* **73**, 023405 (2006).
 [22] J. D. Gillaspay, *J. Phys. B* **34**, R93 (2001).
 [23] J. R. Crespo López-Urrutia, B. Bapat, B. Feuerstein, D. Fischer, H. Lörch, R. Moshhammer, and J. Ullrich, *Hyperfine Interact.* **146/147**, 109 (2003).
 [24] C. Zener, *Phys. Rev.* **36**, 51 (1930).
 [25] J. C. Slater, *Phys. Rev.* **36**, 57 (1930).
 [26] G. Buntkowsky (Universität Jena) (private communication).
 [27] O. E. Alon, V. Averbukh, and N. Moiseyev, *Phys. Rev. Lett.* **80**, 3743 (1998).
 [28] F. Ceccherini and D. Bauer, *Phys. Rev. A* **64**, 033423 (2001).